Uncertainty in vertical extrapolation of measured wind speed via shear

Kelly, Mark; Kersting, Gibson; Mazoyer, Paul ; Yang, Changfeng ; Hernández Fillols, Francisco ; Clark, Steve; Matos, José Carlos

Publication date:
2019

Document Version
Publisher's PDF, also known as Version of record

Uncertainty in vertical extrapolation of measured wind speed via shear

Department of Wind Energy
E Report 2019

Mark Kelly, Gibson Kersting, Paul Mazoyer, Changfeng Yang (杨长锋), Francisco Hernández Fillols, Steve Clark, José Carlos Matos

Dec.2019

DTU Wind Energy E-0195

ISBN 978-87-93549-63-0

DTU Vindenergi
Institut for Vindenergi

Authors: Mark Kelly, Gibson Kersting, Paul Mazoyer, Changfeng Yang (杨长锋), Francisco Hernández Fillols, Steve Clark, José Carlos Matos

Title: Uncertainty in vertical extrapolation of measured wind speed via shear

Department: Wind Energy, Risø Lab/Campus

Summary (max 2000 characters):
This report provides formulations for estimation of uncertainties involved in vertical extrapolation of winds, as well as the total uncertainty incurred when winds observed at one height are extrapolated to turbine hub height for wind resource assessment. This includes new derivations for uncertainties inherent in determination of (wind) shear exponents in both low-shear (offshore) and varying onshore regimes, and subsequent vertical extrapolation of wind speeds. An uncertainty-model validation and check of the constants is also documented, using roughly 80 commercial sites, using objective statistical methods.

A primary motivation for—and part of—this work is the creation of a standard for uncertainty estimation and reporting, which is known as the IEC 61400-15-2. The authors are actively contributing to this emerging standard, and the work herein thus far constitutes (most of) the vertical extrapolation portion of the IEC 61400-15 draft.

ISBN 978-87-93549-63-0
Dec.2019

DTU Wind Energy E-0195
Department of Wind Energy,
Report E-0195

Contract no.:
N/A

Project no.:
N/A

Sponsorship:
The main author received some support from DTU project 44451.

Front page:
Uncertainty in vertical extrapolation of measured wind speed via shear

Pages: 18 (25)
Tables: 0
References: 12

Danmarks Tekniske Universitet
DTU Vindenergi
Risø Campus
Frederiksborgvej 399
Bldg.118/125
4000 Roskilde

www.vindenergi.dtu.dk
Mark Kelly (MKEL@dtu.dk)

Preface

This work gives the details behind the vertical extrapolation portion of the emerging standard for uncertainty estimation and reporting of wind resource assessment, currently known as the IEC 61400-15.
No conflict of interest exists between the main author's DTU affiliation (with e.g. commercial product WAsP) and his IEC role, foremost because the WAsP uncertainty work had been completed in 2012-14 and subsequently published. The remaining authors also do not have a conflict of interest, working together on the 61400-15 for several years together across multiple companies and universities.

Risø Lab/Campus, DTU Wind Energy Dec.2019

Mark Kelly
Senior Scientist, Ph.D.

Contents

Summary

This report provides formulations for estimation of uncertainties involved in vertical extrapolation of winds, as well as the total uncertainty incurred when winds observed at one height are extrapolated to turbine hub height for wind resource assessment. This includes new derivations for uncertainties inherent in determination of (wind) shear exponents in both low-shear (offshore) and varying onshore regimes, and subsequent vertical extrapolation of wind speeds. An uncertainty-model validation and check of the constants is also documented, using roughly 80 commercial sites, using objective statistical methods.

A primary motivation for—and part of—this work is the creation of a standard for uncertainty estimation and reporting, which is known as the IEC 61400-15. The authors are actively contributing to this emerging standard, and the work herein thus far constitutes (most of) the vertical extrapolation portion of the IEC 61400-15 draft.

1. Methodology for calculation of uncertainty due to vertical extrapolation of wind speed

The present methodology to calculate vertical extrapolation uncertainty is limited to vertical extrapolation of observed wind speed (e.g. mean wind speed, Weibull-*A* parameter or reference wind speed) from one (or more) height(s) above ground level, to some height(s) above the measurements. Vertical extrapolation of distribution shape (Weibull-*k*), wind direction, and turbulence intensity are not considered here. For vertical profiles of Weibull-*k* parameter, the reader is directed to e.g. Kelly *et al*. (2014), Troen *et al*. (1987), and Wieringa (1989).

The methodology assumes that vertical extrapolation uncertainty is statistically independent of other uncertainties; i.e., there is no correlation with uncertainties due to horizontal extrapolation, long-term corrections, etc. It can also be assumed that vertical extrapolation uncertainty is normally distributed (Gaussian), allowing combination with other uncertainties and consistent with the Central Limit Theorem. It is recommended to use the appropriate measurement levels that represent the desired calculated variables (hub height wind speed, equivalent rotor wind speed or shear profile across the rotor).

Three methods of vertical extrapolation are commonly used in wind energy (at present, 2019):

- power-law modelling of wind speed profile;
- surface-based wind profile modelling, including surface roughness and the European Wind Atlas (EWA) method; and
- computational fluid dynamics (CFD) modelling via Reynolds-Averaged Navier-Stokes (RANS) solvers.

The first is the most common, and the uncertainty inherent in its use is described in the subsections below. Regardless of the method chosen, a general expression for vertical extrapolation uncertainty should be compatible with the general form

$$\tilde{\sigma}^2_{U,\mathrm{ve}} \simeq k_{s,\mathrm{obs}}\tilde{\sigma}^2_{U_{\mathrm{obs}}} + k_{\mathrm{s,model}}\,\tilde{\sigma}^2_{\mathrm{ind}} \qquad (0)$$

where $\tilde{\sigma}_{U,\mathrm{ve}}$ is the total dimensionless uncertainty associated with vertical extrapolation of wind speed from some height above ground level (observation height) to another (prediction height); the tildes denote dimensionless values (i.e., normalized by expected mean wind speed U, expressible in %). On the right-hand side, $\tilde{\sigma}_{U_{\mathrm{obs}}}$ is the wind speed measurement uncertainty, $\tilde{\sigma}_{\mathrm{ind}}$ is the part of model uncertainty that is independent of the input (measurement) uncertainty, and $k_{\mathrm{s,model}}$ is a coefficient based on the model sensitivity to (one or more) input parameters.

The uncertainty $\tilde{\sigma}_{\mathrm{ind}}$ is part of the (total) model uncertainty, which can be decomposed as

$$\sigma^2_{\mathrm{model}} = \sigma^2_{\mathrm{ind}} + \sigma^2_{\mathrm{mod,ob}}\,; \qquad (1)$$

here $\sigma_{\mathrm{mod,ob}}$ is the observation-dependent part; the coefficient $k_{\mathrm{s,obs}}$ in (0) thus includes sensitivity of the model to measured wind speed. The other contribution σ_{ind} is any remaining model uncertainty that is independent of $\tilde{\sigma}_{U_{\mathrm{obs}}}$.

1.1 Power-law modelling

The mean wind shear exponent (α), defined through the power law wind profile

$$U(z) = U(z_r)\left[\frac{z}{z_r}\right]^{\alpha}, \tag{2}$$

is most directly expressed (e.g. Irwin, 1979; Mikhail, 1985) as

$$\alpha = \frac{dU/dz}{U/z}. \tag{3}$$

Note a *mean* α is specified[1], to vertically extrapolate *mean* wind speed U; this mean is typically defined over 10-minute intervals.[2] We begin by assuming measurements covering an integer number of years. If using a fractional number of years, modification is needed to account for seasonal biases where the latter will tend to increase the uncertainty; the uncertainty in such procedures (e.g. gap-filling and MCP methods) is additional to what we consider here, and can be added within the observational uncertainty used here.

Starting for the simplest case of two measurement heights (z_1, z_2), the centered and theoretically exact formulation (3) is compatible with the commonly used practical form of calculation

$$\alpha = \frac{\ln(U_2/U_1)}{\ln(z_2/z_1)}. \tag{4}$$

Wind shear exponents are assumed to be calculated via (4), using wind speeds averaged over a fixed time interval (standard is 10 minutes, but 30-minutes or more is allowable[3]). These α tend to follow a particular distribution $P(\alpha|U)$ conditional on wind speed, and depend on the height above ground relative to the effective surface roughness (i.e. including terrain complexity; c.f. Kelly *et al.*, 2014a). Regarding the heights used for measurements, it is recommended that they are located within the same atmospheric regime (e.g. *above* the surface layer in shallow nighttime ABLs, or *within* the surface-layer for unstable conditions); for subdivision of data into winter/night-time over land, heights above ~30 m are recommended. The heights used should not be much smaller than the local scale of terrain elevation changes (i.e., the anemometers should not be blocked by hills in commonly occurring wind directions).

In order to minimize the impact and propagation of *systematic* errors (biases) in the vertical extrapolation process, we recommend the following best practices.

- Use of boom-mounted anemometers
  - do *not* use anemometers from different sides of the mast to calculate α, to avoid bias due to tower influence (see section below on correlated systematic errors);
  - do *not* use a 'mix' of top-mounted and boom-mounted anemometers, since mast-top anemometers encounter different flow distortion, leading to bias in calculated α.
- Calibrate all anemometers used (at least on each side of the mast) in the same facility, to avoid bias in the α calculation due to tunnel variability.

---

[1] The shear exponent and associated analysis here is meant for vertical extrapolation, in contrast with α prescribed for site suitability and loads calculations (e.g. IEC 61400-1).

[2] Industrial practice has arrived at an optimal usage of (2), whereby mean wind speeds are extrapolated for each 10-minute interval (Triviño *et al*., 2017); the uncertainty model herein is calibrated for such, as detailed in the next sub-section. One may use e.g. sector-wise and/or monthly means for the extrapolation (instead of 10-minute means), though these tend to result in larger uncertainty, as shown in Triviño *et al*. (2017).

[3] Longer intervals reduce the sampling size, and the ability to measure in different flow regimes. Periods longer than one hour tend to violate statistical stationarity, where the effectiveness of extrapolating each interval becomes degraded.

- All anemometers used (on the same side of the tower should be the same brand and model, to avoid bias in α due to different anemometer responses.

When measurements deviate from the above best practices, the vertical extrapolation uncertainty model will implicitly penalize such arrangements, through propagation of systematic uncertainties.

For the more general case where measurements are available from three or more heights, α can be derived from a least-squares fitting of the mean-wind speed measurements at the different heights. Following the power-law character of (2) this is most directly accomplished in $\ln(V)$ space: a linear fit of $\ln(V)$ versus $\ln(z)$ gives a slope equal to α.

We do not consider changes in the *shape* of the wind distribution with height (such as Weibull-*k* profile, c.f. Kelly *et al*. 2014b) when doing shear-extrapolation; uncertainty in wind power density or AEP is assumed to be treated implicitly via shear calculation per 10-minute sample for power calculations (i.e., through the conditional distribution $P(\alpha|U)$).

Consistent with Eq.1 for σ_{model}, the uncertainty in modelling the (mean) wind shear exponent α at heights above measurements may be expressed as

$$\sigma_{\alpha}^{2} \;=\; \sigma_{\mathrm{rep}}^{2} + \sigma_{\alpha\mathrm{prop}}^{2} + \sigma_{\alpha\mathrm{fit}}^{2} \;; \tag{5}$$

derivation of this is detailed further below (Eqns.13–15). The different terms in (5) account for the representativity of the power law profile, propagation of measurement uncertainty, and potential fitting of the power-law profile to measurements, respectively. Specifically,

- $\sigma_{\mathrm{rep}}^{2}$ characterizes the effect of how well the power law profile—namely its wind shear exponent α derived from observations at some heights—is expected to represent the real wind profile at some prediction height z_{pred} *above* the observation heights;
- $\sigma_{\alpha\mathrm{prop}}^{2}$ is the propagated uncertainty of observations through α;
- $\sigma_{\alpha\mathrm{fit}}^{2}$ is the uncertainty arising, if *fitting* the power-law profile (2) to measurements at *three or more* heights. Monte Carlo simulation can be used to estimate this model-related fitting uncertainty.

Note that (5) also includes the assumption that the fit and representativity are independent of each other; this becomes clearer with the full derivation later.

A preliminary, basic form for σ_{repr} follows from the difference between $\alpha(z_{\mathrm{obs}})$ and $\alpha(z)$ for generalized $\ln(z/z_{0,\mathrm{eff}})$ wind-speed dependence above the surface layer (e.g. Kelly *et al*., 2014a). For the basic power law profile (2), this uncertainty depends primarily upon $(z_{\mathrm{pred}}/z_{\mathrm{obs}})$ and $(z_{\mathrm{pred}}/z_{0,\mathrm{eff}})$, where z_{pred} is the prediction height,

$$z_{\mathrm{obs}} = \exp[\,\textstyle\sum_{i}^{n}(\ln z_i)/n] \;=\; (\,\prod_{i}^{n} z_i\,)^{1/n} \tag{6}$$

is the geometric-mean observation height (e.g. $z_{\mathrm{obs}} = \sqrt{z_1 z_2}$ for 2 heights), and $z_{0,\mathrm{eff}}$ is an effective roughness length corresponding to the terrain over which the shear was measured. By adapting the roughness-change length scale of Fourier z_0-response modelling (Astrup & Larsen, 1999), using σ_z as the effective surrogate for the outer spectral scale, one has

$$z_{0,\mathrm{eff}} = [z_0(\sigma_z + z_0)^2]^{1/3} \tag{7a}$$

where z_0 is the surface roughness length, and σ_z is the standard deviation of terrain elevation extending 3 km upwind[4]. If lacking σ_z, the crude relation $\mathrm{RIX} \sim a_R \ln(1 + \sigma_z \,/\, \Delta z_{\mathrm{ref}})$ can be employed to relate RIX (in %) to σ_z, where the constant $a_R \approx 30\%$ and $\Delta z_{\mathrm{ref}} \approx 100\mathrm{m}$ for a range of complex-to-moderate terrain types; then an effective roughness length can be calculated via

$$\mathrm{z}_{0,\mathrm{eff}} \simeq \mathrm{z}_0\left[1 + \Delta \mathrm{z}_{\mathrm{ref}}\,(\mathrm{e}^{\mathrm{RIX}/a_R} - 1)/\mathrm{z}_0\right]^{2/3} . \tag{7b}$$

Using $\ln\left(z/z_{0,\mathrm{eff}}\right) = \ln(z/z_{\mathrm{obs}}) + \ln\left(z_{\mathrm{obs}}/z_{0,\mathrm{eff}}\right) = \ln(z/z_{\mathrm{obs}}) + \alpha_{\mathrm{obs}}^{-1}$, one obtains a simple estimate for the dimensionless uncertainty due to (lack of) representativeness of the observed shear exponent α_{obs} at a height z different than observation height z_{obs} :

$$\tilde{\sigma}_{\mathrm{rep}} = \frac{\alpha_{\mathrm{obs}} - \alpha_{\mathrm{eff}}\left(z, z_{0,\mathrm{eff}}\right)}{\alpha_{\mathrm{eff}}\left(z, z_{0,\mathrm{eff}}\right)} = \alpha_{\mathrm{obs}} \ln\left(z_{\mathrm{pred}}/z_{\mathrm{obs}}\right).$$

In the above and hereafter, the over-tilde denotes non-dimensional quantities; i.e., normalized by the (predicted) mean variable described by the σ (in this case wind speed), expressible also as a percentage divided by 100.

The above expression for $\tilde{\sigma}_{\mathrm{rep}}$ does not account for complex flow conditions, where the shear can be significantly decreased due to e.g. hill-induced mixing: when the observed shear exponent is small such that $\alpha(\mathrm{z}_{\mathrm{obs}}) \ll 1/\ln\left(\mathrm{z}_{\mathrm{obs}}/\mathrm{z}_{0,\mathrm{eff}}\right)$, then the measurements are in effect too close to the ground (relative to the local variations in terrain elevation) to do reliable shear-based extrapolation, and α varies significantly with height z. In such cases the estimate for $\tilde{\sigma}_{\mathrm{rep}}$ above results in underestimation. Thus, to estimate $\tilde{\sigma}_{\mathrm{rep}}$ we use a heuristic model to account for the increase in uncertainty over complex terrain, via the factor

$$B_{\mathrm{ct}} = \frac{c_r}{\ln\left(\sqrt{\mathrm{z}_{\mathrm{pred}}\mathrm{z}_{\mathrm{obs}}}/\mathrm{z}_{0,\mathrm{eff}}\right)} ; \tag{8}$$

this gives

$$\tilde{\sigma}_{\mathrm{rep}} \simeq \; B_{\mathrm{ct}}\,\alpha \ln\left(\frac{z_{\mathrm{pred}}}{z_{\mathrm{obs}}}\right) = \; c_r \frac{\alpha \,\ln\left(z_{\mathrm{pred}}/z_{\mathrm{obs}}\right)}{\ln\left(\sqrt{z_{\mathrm{pred}}z_{\mathrm{obs}}}/z_{0,\mathrm{eff}}\right)} . \tag{9}$$

The coefficient c_r is expected to be of order 1; initially we empirically find c_r~2, through analysis of data from several dozen sites of different complexity.

However, for offshore conditions (and some less common land cases) the observed shear exponent may be so small (especially $\alpha \lesssim 0.1$) that (9) underpredicts $\tilde{\sigma}_{\mathrm{rep}}$ due to advective and top-down (finite-ABL)[5] effects. For example, in these regimes, for measurement heights above 50 m and hub heights of 100 m over water, (9) predicts $\tilde{\sigma}_{\mathrm{rep}} < 1\%$; this is contrary to observed errors.

---

[4] The adaptation of spectral roughness-change length scale is also consistent with e.g. Anderson & Meneveau (2011). The calculation limit of 3 km upwind corresponds to both the scale of 3.5 km in the empirical definition of RIX, and the scale separating terrain-spectra regimes (Beljaars, 2004); a spatial weighting function could allow calculating σ_z over a larger area, but this is an active area of research.

[5] The finite depth of the atmospheric boundary layer (ABL), when low enough to be comparable turbine upper-tip heights (e.g. winter or night-time), can cause both high and low shear anomalies through e,g, the high shear above and jets associated with such.

A low-shear correction of the form $e^{-\alpha/\alpha_{\mathrm{ref}}}$ follows observed extrapolation statistics and *could* be added to (9), but since the contribution due to $\tilde{\sigma}_{\mathrm{rep}}$ will be multiplied by $\alpha \ln(z_{\mathrm{pred}}/z_{\mathrm{obs}})$ in the total uncertainty (as seen below), the corrective form must be made practical such that the contribution to total uncertainty does not vanish as $\alpha \to 0$. A correction satisfying these criteria (equivalent to $e^{-\alpha/\alpha_{\mathrm{ref}}}$ for $\alpha \gtrsim \alpha_{\mathrm{ref}}$ but better-behaved) is

$$B_{os}[1 + \tanh(-\alpha/\alpha_{\mathrm{ref}})] \times |\alpha|^{-1}.$$

The representativeness uncertainty subcomponent can thus be written accounting for both low-shear and complex-terrain conditions as

$$\tilde{\sigma}_{\mathrm{rep}} \simeq B_{ct}\alpha \ln\left(\frac{z_{\mathrm{pred}}}{z_{\mathrm{obs}}}\right) + B_{os}|\alpha|^{-1}[1 + \tanh(-\alpha/\alpha_{\mathrm{ref}})]\,. \tag{10}$$

Initial tests over low-shear sites suggested $\alpha_{\mathrm{ref}} = 0.2$; validating expression (10) against ~80 sites including both low- and high-shear wind climates in various offshore and onshore locations with different complexity, we further find that $B_{os} = 0.04$ is optimal along with $c_r \simeq 2$ in Eq.8. Details of the validation are shown in the next subsection.

For measurements at 2 heights, an approximate dimensionless form can be derived for the propagation of measurement uncertainty in the determination of α, via the differential of (4) and standard error propagation analysis (e.g. GUM):

$$\delta \ln \alpha \simeq \frac{\delta(\ln U_2 - \ln U_1)}{\alpha \ln(z_2/z_1)}$$

ignoring the uncertainty in measurement heights, which leads to

$$\tilde{\sigma}_{\alpha\mathrm{prop}} \simeq \frac{\sqrt{\tilde{\sigma}^2_{U,\mathrm{obs}}|_{z_1} + \tilde{\sigma}^2_{U,\mathrm{obs}}|_{z_2}}}{\alpha \ln(z_2/z_1)} \approx \frac{c_f}{\ln(z_2/z_1)}\frac{\tilde{\sigma}_{U,\mathrm{obs}}}{\alpha}\,. \tag{11}$$

Again, the tildes denote normalized/non-dimensional quantities (i.e. percentage divided by 100), and $\tilde{\sigma}_{U_{\mathrm{obs}}}$ is the normalized uncertainty in observation (calculated elsewhere). The coefficient c_f is monotonic in the correlation between observational uncertainty at the different anemometers; it can also be adjusted to account for special conditions where the mean wind profile is known to deviate significantly from logarithmic or power-law forms. Assuming the same uncertainty for each anemometer and no correlated observational uncertainties between anemometers, then $c_f = \sqrt{2}$ for the case of two anemometers. Note that the sub-component $\tilde{\sigma}^2_{\mathrm{prop}}$ is part of the measurement uncertainty term $k_{\mathrm{s,obs}}\tilde{\sigma}^2_{U_{\mathrm{obs}}}$ in the general uncertainty form (0).

1.1.1 Using 3 or more heights for extrapolation

The propagation term (11) was derived for 2 heights. When one uses more than 2 measurement heights, the wind shear exponent can be derived from fitting the wind speed measurements at the different heights. This is directly accomplished via least-squares fitting in $\{\ln(z), \ln(V)\}$ space: a linear fit of $\ln(V)$ versus $\ln(z)$, where the slope is then α. Then an alternate to (11) is needed, as well as the uncertainty $\sigma^2_{\alpha\mathrm{fit}}$ in fitting the shear-profile. The representativeness term $\tilde{\sigma}_{\mathrm{rep}}$ is again calculated by (6), where the effective observation height z_{obs} for *n* heights is given by[6]

[6] For *n* heights, assuming each observation height has equal weight in the Monte-Carlo profile fitting. For unequal weights, (12) can be modified by replacing 1/*n* with the individual weights w_k.

$$z_{\text{obs}} = \exp\left[\frac{1}{n}\sum_k^n \ln z_k\right] = \left(\prod_k^n z_k\right)^{1/n}. \quad (12)$$

A Monte Carlo simulation (or similar method) can also be used to estimate the fitting uncertainty $\sigma^2_{\alpha\text{fit}}$, as well as the observational uncertainty propagation; the latter replaces (11). From Monte-Carlo simulations based on the measurement uncertainties at the different heights, following GUM (JCGM 100, JCGM 101), the normalized uncertainty $\tilde{\sigma}_{\alpha\text{fit}}$ is that due to fitting the mean profile. This can be calculated using least-squares fitting of ln[*V*] versus ln[*z*] (e.g. JCGM 101). Then, instead of using $k_{s,\text{obs}}$ from (11) , the first term $k_{s,\text{obs}}\tilde{\sigma}^2_{U_{\text{obs}}}$ in (0) is replaced by the component of Monte-Carlo output variance due to propagated random observational uncertainty (i.e., $k_{s,\text{obs}}$ is in effect the ratio of dimensionless propagated variance to square of aggregate measurement uncertainty). The Monte-Carlo estimate of the propagation term for $n \geq 3$ tends to be smaller than the $n = 2$ estimate from (11), compensating for the addition of the profile-fit uncertainty $\tilde{\sigma}_{\alpha\text{fit}}$, but use of more than 2 heights can either decrease or increase the uncertainty, particularly because lower measurement heights tend to contribute less representative information with regard to hub-height prediction.[7]

Without doing Monte-Carlo calculations, a cruder adjustment for 3–5 heights is to simply multiply the result of (11) by $\sqrt{2/n}$, where n is the number of measurement heights.

1.2 Total extrapolation uncertainty

To obtain the uncertainty in power law profile extrapolation of mean wind speed, the propagation of measurement uncertainty must be incorporated properly with the uncertainty of modelling the wind shear exponent. Applying (2) for extrapolating U_{obs} to U_{pred} and taking the differential, one obtains

$$\delta U_{\text{pred}} = \frac{U_{\text{pred}}}{U_{\text{obs}}}\delta U_{\text{obs}} + U_{\text{pred}} \ln\left(\frac{z_{\text{pred}}}{z_{\text{obs}}}\right)\delta\alpha + \alpha\left(\frac{\delta z_{\text{pred}}}{z_{\text{pred}}} - \frac{\delta z_{\text{obs}}}{z_{\text{obs}}}\right)U_{\text{pred}} \ . \quad (13)$$

Rewriting this non-dimensionally as

$$\delta \ln U_{\text{pred}} = \delta \ln U_{\text{obs}} + \ln\left(z_{\text{pred}}/z_{\text{obs}}\right)\delta\alpha + \alpha\left(\delta \ln z_{\text{pred}} - \delta \ln z_{\text{obs}}\right) ,$$

then squaring and retaining lowest-order terms (i.e. excluding cross-correlation terms as well), leads to an expression for non-dimensional uncertainty ($\tilde{\sigma}_{U_{\text{pred}}}$, i.e. fraction of U_{pred}) in mean wind speed due to power-law profile extrapolation. Noting that $U(z_{\text{ref}})$ is actually $U(z_n)$ for the case of *n* measurement heights, the total normalized uncertainty is expressed in terms of dimensionless component uncertainties as

$$\tilde{\sigma}^2_{U_{\text{pred}}} \simeq \tilde{\sigma}^2_{U_{\text{obs},n}} + \alpha^2\tilde{\sigma}^2_{\alpha}\left[\ln\left(z_{\text{pred}}/z_{\text{obs}}\right)\right]^2 + \alpha^2\tilde{\sigma}^2_{z_{\text{obs}}} \ . \quad (14)$$

The first term on the right-hand side of (14) is the 'directly' propagated uncertainty in wind measurement at the top height (e.g. $\tilde{\sigma}^2_{U_{\text{obs},2}}$ if using 2 heights) due to the latter appearing outside of α in (2); again, $\sigma^2_{\alpha} = \alpha^2\tilde{\sigma}^2_{\alpha} = \alpha^2(\sigma^2_{\text{rep}} + \sigma^2_{\alpha\text{prop}} + \sigma^2_{\alpha\text{fit}})$ is the dimensional squared uncertainty

[7] The representativity expression (6) will tend to compensate for the effect of using more heights which are lower, because the shear tends to increase approaching the ground (at least over simpler terrain). However, the uncertainty model is not explicitly designed to account for the possibility of increased uncertainty due to using more heights.

of obtaining the shear exponent following (4)[8]. The final term of (14) is the contribution from uncertainty in measurement heights. Using (11) for $\sigma^2_{\alpha\mathrm{prop}}$, and neglecting the dimensionless uncertainty in measurement height, the total vertical extrapolation uncertainty can be expanded and re-written for the case of 2 measurement heights as

$$\tilde{\sigma}^2_{U_{\mathrm{pred}}} \simeq \tilde{\sigma}^2_{U_{\mathrm{obs}}}\left[1+\left(c_f\frac{\ln\left(\mathrm{z_{pred}}/z_{\mathrm{obs}}\right)}{\ln(z_2/z_1)}\right)^2\right]+\alpha^2\tilde{\sigma}^2_{\mathrm{rep}}\left[\ln\left(\mathrm{z_{pred}}/z_{\mathrm{obs}}\right)\right]^2 \quad , \tag{15}$$

again with σ^2_{rep} from (10). The contribution due to uncertainty in measurement heights ($\alpha^2\tilde{\sigma}^2_{z_{\mathrm{obs}}}$) is neglected because it is typically much smaller than the other terms: $\tilde{\sigma}_{z_{\mathrm{obs}}}$ rarely exceeds 1%, and $\alpha^2 \ll 1$ for conditions where shear-extrapolation can be used. One possible exception is displaced flow over e.g. forests, where $\tilde{\sigma}_{z_{\mathrm{obs}}}$ might be on the order of 10% in effect, though α still tends to be small enough to neglect $\tilde{\sigma}_{z_{\mathrm{obs}}}$ unless the local climate is heavily dominated by stable conditions.[9]

Thus far the component uncertainties have been considered to be random. However, the measurement uncertainty may contain a systematic component, i.e., measurement bias; the square of this ($\tilde{b}^2_{U\mathrm{obs}}$) can be added to (15). In contrast to the random uncertainties, due to the character of upward extrapolation via the power law, for the case of *un*correlated biases across anemometers an *additional* systematic uncertainty $2\tilde{b}^2_U\left[\frac{\ln\left(\mathrm{z_{pred}}/z_{\mathrm{obs}}\right)}{\ln(z_2/z_1)}\right]^2$ is propagated (see Appendix A.2 for details). Thus the propagation term $\sigma^2_{\alpha\mathrm{prop}}$ simply has an additional component resembling the random component, but with $2\tilde{b}^2_{U\mathrm{obs}}$ instead of $c_f^2\tilde{\sigma}^2_{U_{\mathrm{obs}}}$.

Within the context of the generic formulation (0), which partitions the total vertical extrapolation uncertainty into an observation-related component $k_{s,\mathrm{obs}}\tilde{\sigma}^2_{U_{\mathrm{obs}}}$ and an independent component $k_{\mathrm{s,model}}\,\tilde{\sigma}^2_{\mathrm{ind}}$, comparing with (15) we can write the respective sensitivity coefficients for the random uncertainty as

$$k_{s,\mathrm{obs}} \simeq \left(c_f\frac{\ln\left(\mathrm{z_{pred}}/z_{\mathrm{obs}}\right)}{\ln(z_2/z_1)}\right)^2 \quad ; \quad k_{\mathrm{s,model}} = \left[\alpha\ln\left(\mathrm{z_{pred}}/z_{\mathrm{obs}}\right)\right]^2 \quad , \tag{16}$$

with $\tilde{\sigma}^2_{\mathrm{ind}} = \tilde{\sigma}^2_{\mathrm{rep}}$ in (0).

Overall, the approach outlined here can be applied per sector, summing frequency- or energy-weighted $\tilde{\sigma}^2_{U_{\mathrm{pred}}}$. Further, such weighted calculations can also be used on a seasonal or diurnal basis.

[8] One could also include the Weibull-weighted effect of the mean wind-speed dependence that arises from the width of $P(\alpha|U)$ being inversely proportional to U [Kelly *et al.*, 2014a]; this is appropriate if using yearly-mean (not 10-minute) α.

[9] There are also situations where remote-sensing devices (such as lidar, sodar, or radar) can have non-negligible $\alpha^2\tilde{\sigma}^2_{z_{\mathrm{obs}}}$; however, such measurements are usually used at hub-height, not for extrapolation. One may add this piece if using e.g. lidar with extrapolation, if it is significant.

2. Validation

There are two constants within the representativeness subcomponent, which needed to be tuned empirically; these are the coefficient c_r in the complex-terrain correction factor B_{ct} (8), and the constant B_{os} within the low-shear/well-mixed site adjustment going into (10). Without the low-shear adjustment, we found $c_r \simeq 2$, but expected this to potentially change due to addition of the low-shear correction.

Including the low-shear correction, we find the optimal values $B_{os} = 0.04$ and again $c_r \simeq 2$. Figure 1 displays the difference between dimensionless estimated uncertainty $\tilde{\sigma}^2_{U_{\mathrm{pred}}}$ from (14) and absolute extrapolation error $|\tilde{\epsilon}_U|$ for these $\{B_{os}, c_r\}$ and the ~80 sites analyzed. Figure 1 also includes $\tilde{\epsilon}_U$ itself, to show the general trend of extrapolation error versus shear. The figure basically shows the performance of the uncertainty estimation model, with the difference between predicted uncertainty (not error) and absolute error being smaller than the error at most sites; for Gaussian-distributed errors, the constants should be calibrated such that roughly 4 sites should have errors which exceed the uncertainty predictions (see Appendix).

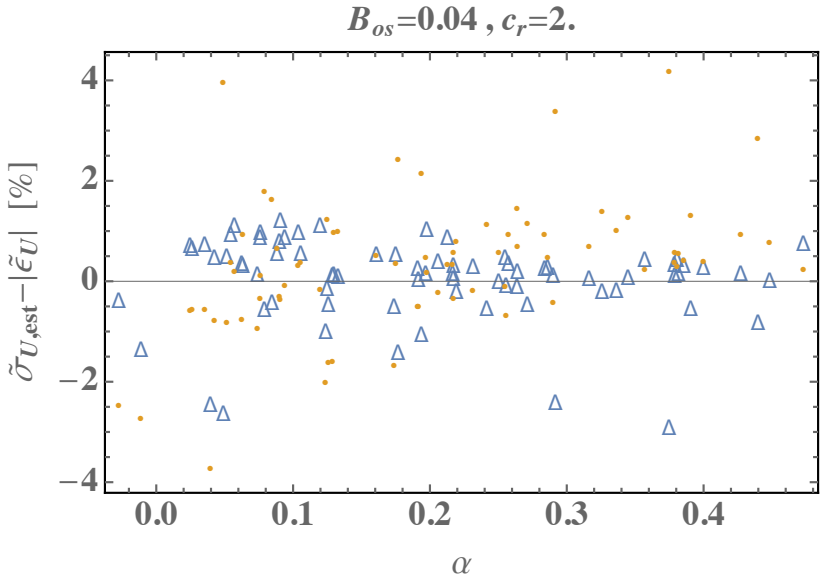

Figure 1. Difference between estimated uncertainty σ_U from (14) and observed absolute wind-speed error $|\epsilon_U|$ due to shear extrapolation (blue triangles) versus shear exponent; yellow dots show ϵ_U.

Over all (~80) the sites analyzed, the distribution of mismatch between predicted uncertainty and error in predicted wind speed via shear extrapolation ($\tilde{\sigma}^2_{U,est} - |\tilde{\epsilon}_U|$, shown versus α in Figure 1) is displayed in Figure 2 as a histogram, again for the optimal parameters $B_{os} = 0.04$ and $c_r = 2$.

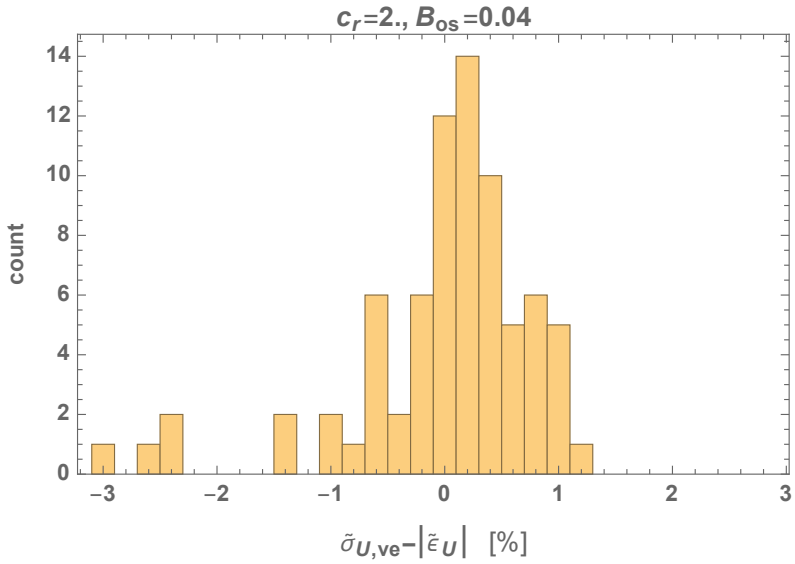

Figure 2. Histogram of difference between estimated uncertainty using (14) and observed absolute error in wind speed due to shear extrapolation, for the optimal parameters $B_{os} = 0.04$ and $c_r = 2$.

One can see in Figure 2 that the most common values of the difference between estimated uncertainty and absolute error are centered around 0, but slightly positive (< 0.3%); the positivity compensates for several underpredicted 'outliers'. The main justification for the choice of extrapolation-uncertainty model parameters is based on minimizing the mean difference between modelled uncertainty and observed absolute error ($\tilde{\sigma}^2_{U,est} - |\tilde{\epsilon}_U|$).

Further justification for the choice of optimal parameters is seen in Figure 3, which displays the magnitude of the mean of the 'mismatch' ($\tilde{\sigma}^2_{U,est} - |\tilde{\epsilon}_U|$) over all sites, for different values of B_{os} and c_r; it corresponds to taking the mean of thousands of distributions like that shown in Figure 2, for B_{os} spanning a range from 0.01 to 0.08 and c_r ranging from 0.5 to 3.0.

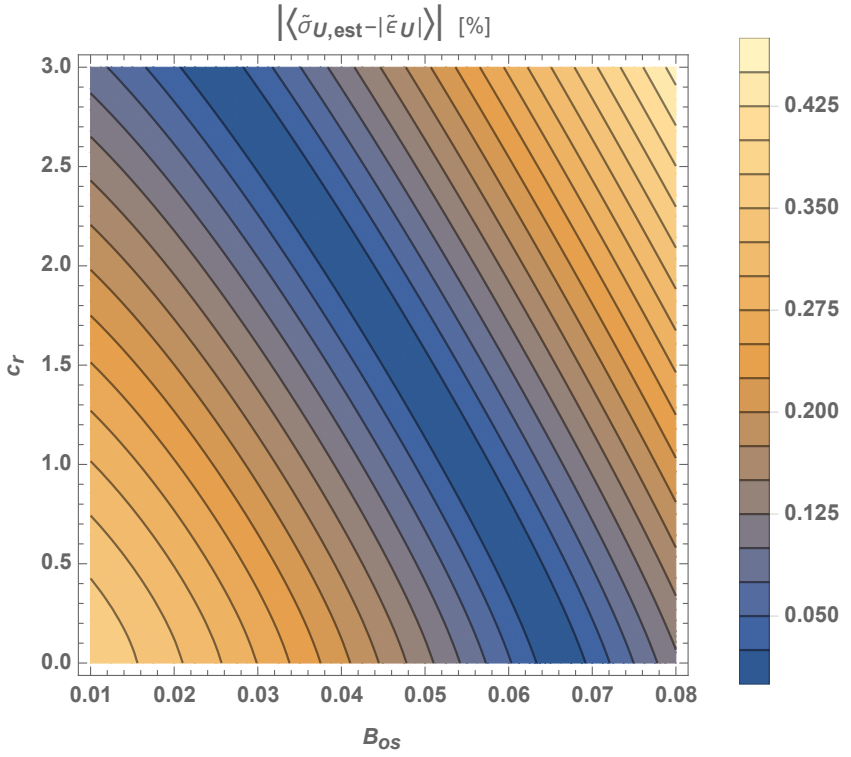

Figure 3. Magnitude of mean difference between uncertainty estimate and observed absolute error in vertical extrapolation, for different values of the uncertainty-model constants.

One can see in Figure 3 that a curve of $\{B_{os}\,, c_r\}$ gives minimal mismatch between estimated uncertainty and absolute extrapolation error; e.g. for values $B_{os} = 0.05$ and $c_r \simeq 1.5$ one obtains similar mean errors, though this does not handle low-shear outliers as well. Although it is also possible to calibrate these constants to e.g. the median of $(\tilde{\sigma}_{u,\text{est}} - |\tilde{\epsilon}_U|)$, we avoid doing so; since the median is focused on the most common values, it tends to discount the effect of (ignore) the high-error projects.

Regarding the outliers and calibration of the constants, one can also consider the width of the dimensionless error distribution $p(\tilde{\epsilon}_U)$, which has been assumed to be Gaussian. This was first done for the single constant B_{os} in the low-shear adjustment, as shown in the Appendix. Basically, for a Gaussian error distribution, one expects the error to sometimes randomly exceed the uncertainty; i.e. one expects the error $\tilde{\epsilon}_U$ to exceed $\sigma_{\tilde{\epsilon}_U}$ for 31.7% of cases, and one expects a 10% exceedance rate for a value of $\tilde{\epsilon}_U$ that is 1.28 times this. The low-shear cases (Appendix) gave the value $B_{os} = 0.04$ for uncertainty estimates of the 90th percentile; from Figure 3 one can see $c_r = 2$ follows.[10]
One can also see that our choice of constants minimizes error in uncertainty prediction, by examining the standard deviation of $(\tilde{\sigma}_{u,\text{est}} - |\tilde{\epsilon}_U|)$ over all cases, again using large ranges of c_r and B_{os}; this displayed in Figure 4.

[10]Alternately a larger value of $B_{os} = 0.055$ is obtained for the 68th ["1σ"] percentile, and then $c_r \simeq 1.5$.

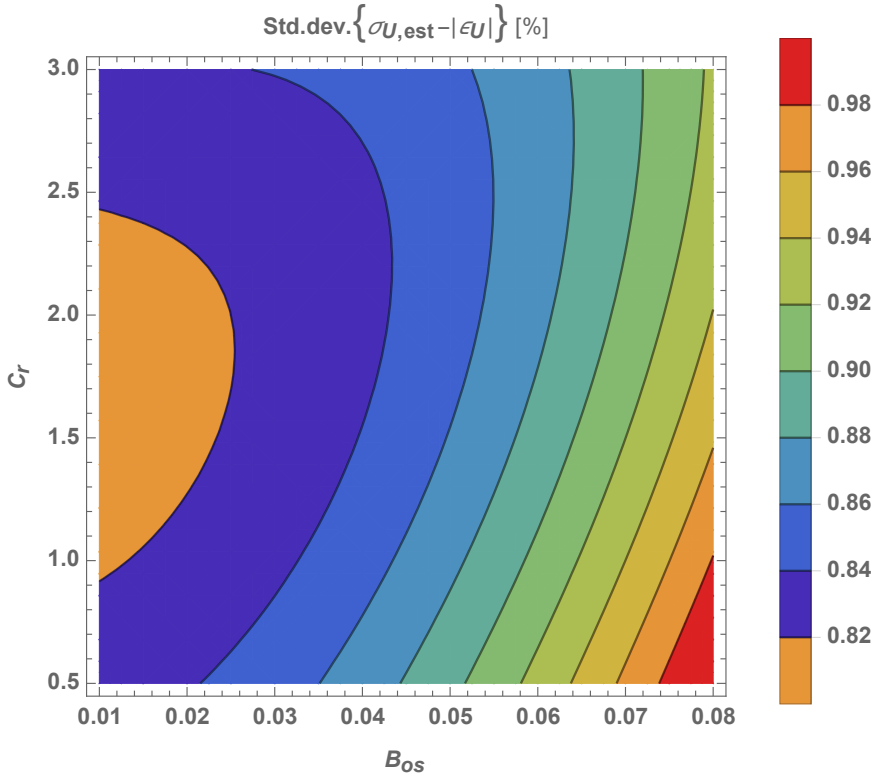

Figure 4. Standard deviation of difference between estimated uncertainty using (14) and observed error at all sites considered, for different values of complex-terrain coefficient c_r and low-shear constant B_{os}.

Also notable from Figure 4 is that the variability of difference between dimensionless uncertainty and absolute observed error is smaller for the 90th-percentile uncertainty prediction (which uses $B_{os} = 0.04$ and $c_r \simeq 2$), than that obtained using the constants found for the 68th-percentile ("1 sigma") uncertainty prediction ($B_{os} = 0.05$ and $c_r \simeq 1.5$).

We recommend use of the 90th-percentile coefficients, both because of the need to also account for some rarer cases, and also because of the improved (reduced) variability of the predicted-to-observed difference evidenced in Figure 4.

Appendices

A.1. Correction to representativeness subcomponent in low-shear conditions

From the many-site observations given by EON and GoldWind, we saw that the model was underpredicting uncertainty relative to the observed error at offshore low-shear sites; this is because the $\tilde{\sigma}_{\text{rep}}$ model is α-dependent, to account for variation of shear with height due to classical 'bottom-up' (roughness-like) effects (whereas offshore the complex-terrain part doesn't matter).

For low-shear sites ($\alpha < 0.2$) the observed dimensionless error in extrapolated wind speed as a function of α (left plot), and the 'simply' predicted uncertainty (right plot) look like:

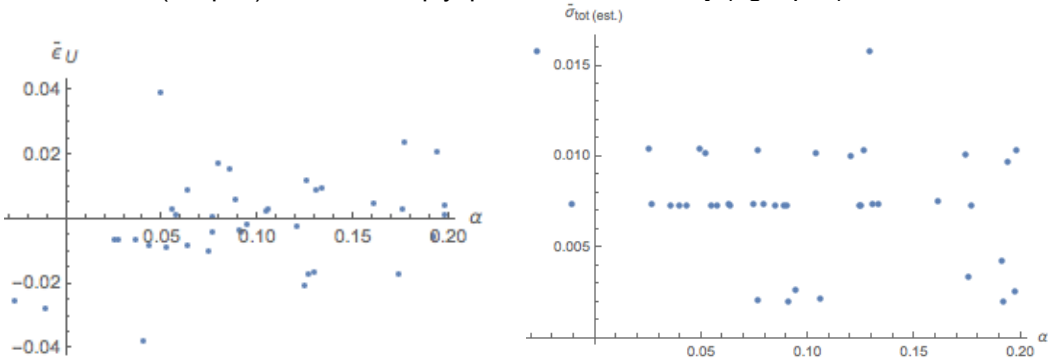

i.e., the 'simply' predicted uncertainty (<1.6%) is lower than the observed error ($|\tilde{\epsilon}|$ up to 4%).

EON/GoldWind provided a dataset containing the shear exponent α, error $\tilde{\epsilon}$, the $\tilde{\sigma}_{\text{rep}}$, profile-fitting subcomponent $\tilde{\sigma}_{\text{fit}}$, also the representativeness contribution $[\tilde{\sigma}_{\text{rep}}\alpha \ln(z_{pred}/z_{obs})]$ to vertical extrapolation uncertainty $\tilde{\sigma}_{\text{ve}}$, and finally the total estimated $\tilde{\sigma}_{\text{ve}}$.

Recall that the vertical extrapolation uncertainty follows

$$\tilde{\sigma}^2_{U_{\text{ve}}} \simeq \frac{\tilde{\sigma}^2_{U_{\text{obs}}}\big|_{z_1} \ln^2(z_{\text{pred}}/z_2) + \tilde{\sigma}^2_{U_{\text{obs}}}\big|_{z_2} \ln^2(z_{\text{pred}}/z_1)}{\ln^2(z_2/z_1)} + \alpha^2\left(\tilde{\sigma}^2_{\text{rep}} + \tilde{\sigma}^2_{\alpha\text{fit}}\right)\left[\ln\left(z_{\text{pred}}/z_{\text{obs}}\right)\right]^2 ,$$

where $\tilde{\sigma}^2_{U_{\text{pred}}} \simeq \tilde{\sigma}^2_{U_{\text{obs}}} + \tilde{\sigma}^2_{U_{\text{ve}}}$); this implies $\tilde{\sigma}^2_{\text{ind}} = \tilde{\sigma}^2_{\text{rep}} + \tilde{\sigma}^2_{\alpha\text{fit}}$ in the general expression for vertical extrapolation uncertainty from the main text,

$$\tilde{\sigma}^2_{U,\text{ve}} \simeq k_{\text{s,obs}}\tilde{\sigma}^2_{U_{\text{obs}}} + k_{\text{s,model}}\tilde{\sigma}^2_{\text{ind}} , \qquad (0)$$

with a sensitivity coefficient of $k_{\text{s,model}} = \alpha^2\left[\ln\left(z_{\text{pred}}/z_{\text{obs}}\right)\right]^2$.

For anemometers having equal measurement uncertainties and no correlated uncertainty between them, then the first term on the right-hand side of (11) reduces to give the effective measurement sensitivity coefficient of $k_{\text{s,obs}} = [\ln^2(z/z_2) + \ln^2(z/z_1)]/\ln^2(z_2/z_1)$ following (0).

One can use (11) to infer $\tilde{\sigma}^2_{\mathrm{rep}}$ from $\tilde{\sigma}^2_{U_{\mathrm{ve}}}$, given the other terms. Here we used the 'envelope' of largest $\tilde{\epsilon}$ as a proxy for $\tilde{\sigma}^2_{U_{\mathrm{ve}}}$; note that this itself involves some uncertainty since we are thus taking the envelope of the dataset's $\tilde{\epsilon}$ to correspond to $1 \cdot \tilde{\sigma}^2_{U_{\mathrm{ve}}}$. The data did not include explicit $\{\mathrm{z}_1, \mathrm{z}_2\}$, however this was estimated by using the $\ln(\mathrm{z}_{\mathrm{pred}}/z_{\mathrm{obs}})$ contained in the dataset along with a prediction height around 100m; thus the $k_{\mathrm{s,obs}}$ coefficient on $\tilde{\sigma}^2_{U_{\mathrm{obs}}}$ in (11) is estimated to be equal to 10 on average, and the equation is solved for $\tilde{\sigma}^2_{\mathrm{rep}}$. Doing so for the low-shear cases, we have the following result (blue dots):

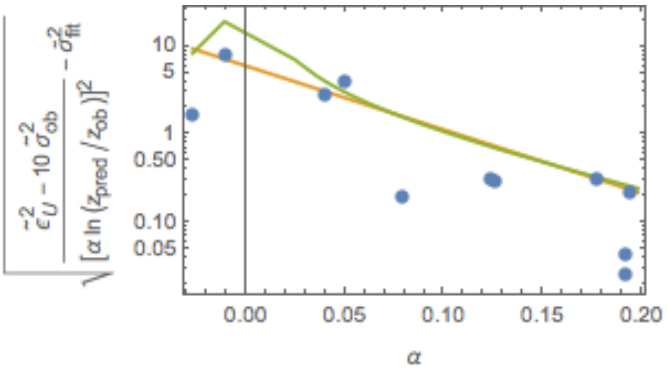

where one can see that many of the low error cases are not depicted, because the root becomes imaginary. This is acceptable because we are really considering the largest error cases. Crudely (and analogous to/extending e.g. Beljaars, 2004), the form $\exp(-\alpha/\alpha_{\mathrm{ref}})$ fits the largest inferred $\tilde{\sigma}_{\mathrm{rep}}$, as shown by the yellow line in the above figure. This form has the property that more negative values of shear are 'penalized.' However, since $\tilde{\sigma}_{\mathrm{rep}}$ is multiplied by α in (11), then such a form will give spuriously zero contribution to the total as $\alpha \to 0$. A form which also fits but rectifies this problem is

$$B_{os}\exp(-\alpha/\alpha_{\mathrm{ref}}) \times |\alpha|^{-1} \qquad \text{(A1)}$$

where $B_{os} = 0.2$ and $\alpha_{\mathrm{ref}} = 0.13$; this is shown by the green line. The equivalent form without $1/\alpha$ (yellow line) is $30B_{os}\exp(-\alpha/0.45\alpha_{\mathrm{ref}})$.

Below the two forms are shown added to the original $\tilde{\sigma}_{\mathrm{rep}}$ (black).

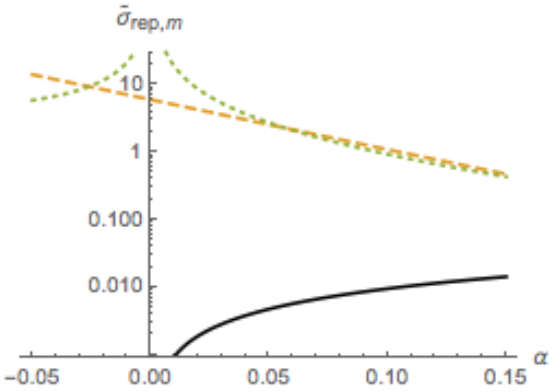

Multiplying by $\alpha \ln(z_{pred}/z_{obs})$, we can see the functions as their contribution to $\tilde{\sigma}_{\mathrm{ve}}$, below.

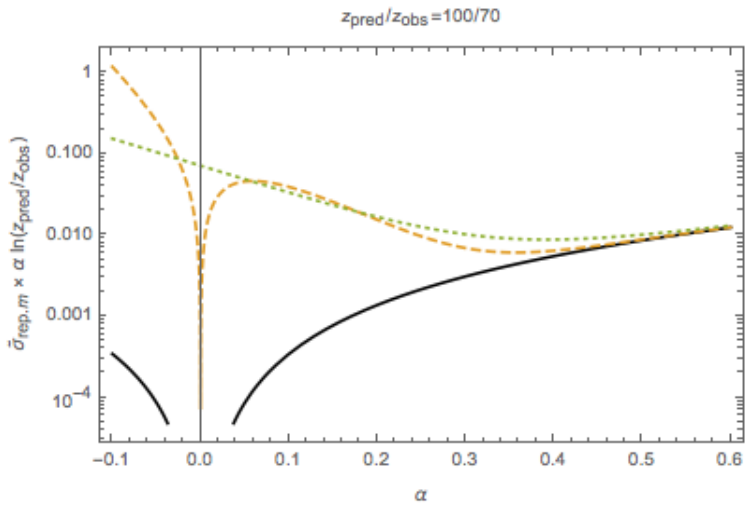

Thus one can see the second form gives a continuous contribution across zero shear, increasing for negative shear.

The result of using the new form (A1) and the simpler exponential form to calculate $\tilde{\sigma}_{\mathrm{ve}}$ are shown below.

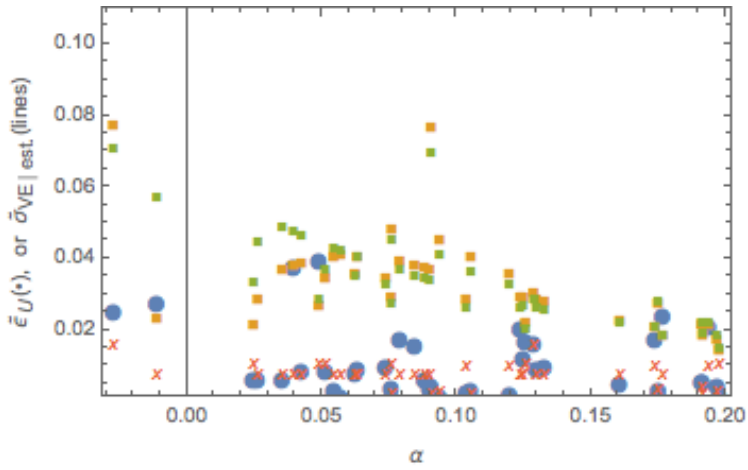

The blue dots are the observed errors in predicted (extrapolated) wind speed, the yellow squares are the simpler exp form, and the green squares are $\tilde{\sigma}_{\mathrm{ve}}$ using the adapted form (6a). One can see the green dots falling just above the most 'extreme' outliers for positive shear, while for negative shears the estimate appears more conservative. However, recall that negative shear is generally not expected to persist upwards with height; the 2 data points are likely not so extreme.

To be less conservative (but a little more complicated), a similar form which gives 'less conservative' estimates relative to this dataset, but which also gives a smaller variation on the negative side (and matches the exponential form for $\alpha > \sim 3\alpha_{\mathrm{ref}}$), is

$$B_{os}[1 + \tanh(-\alpha/1.5\alpha_{\mathrm{ref}})] \times |1.3\alpha|^{-1}. \qquad \text{(A2)}$$

This can be seen by the red line of the first plot below, and by the green "*T*" markers in the results plotted second.

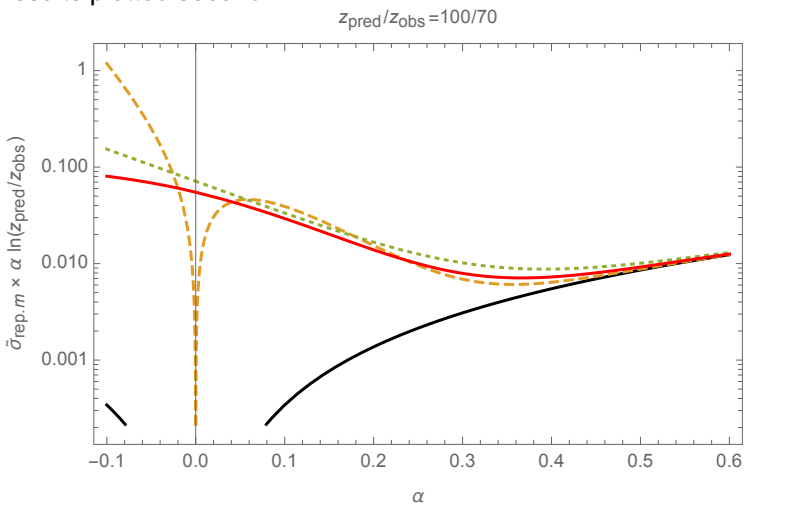

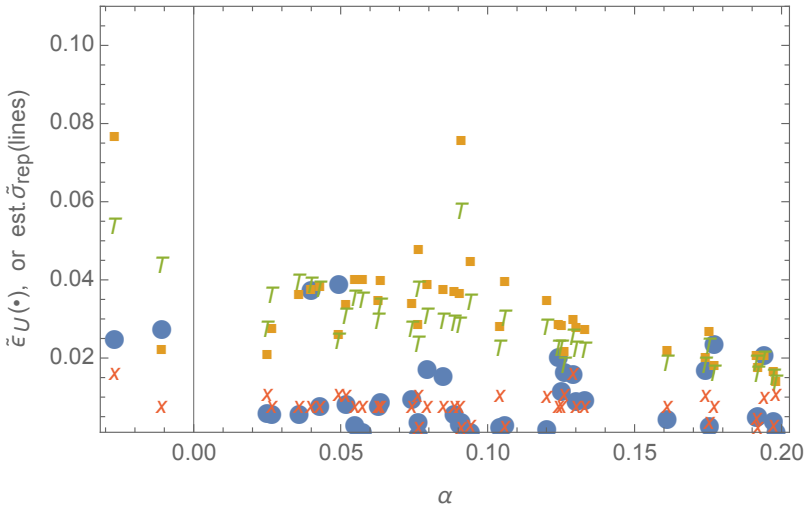

Note that the form (A2) can be made to look simpler if we do use it, by absorbing the factors 1.3 and 1.5 into the coefficients B_{os} and α_{ref}, i.e. updating them to 0.15 and 0.2 respectively to simply write $B_{os}[1 + \tanh(-\alpha/\alpha_{\mathrm{ref}})] \times |\alpha|^{-1}$.

However, we must account for the expected error distribution width, regarding our calibration of the coefficient B_{os}. Some of the observed errors are rarer cases that likely occur less frequently than what one would expect from a normal distribution. For normally distributed errors, one expects 31.7% of samples to have $\tilde{\varepsilon} > \tilde{\sigma}_{\mathrm{rep}}$. Since there are not a large number of samples per α-bin, we must calibrate B_{os} using all the samples. For the 40 cases here, one then expects 12 samples to exceed $\tilde{\sigma}_{\mathrm{rep}}$; a value of $B_{os} = 0.055$ returns such a result, as seen in the next plot below.

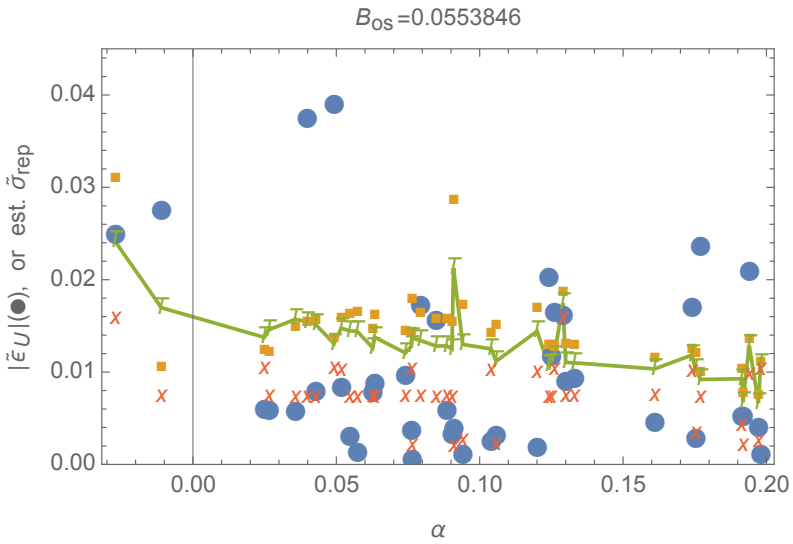

The contribution to total shear looks like the plot on the previous page, but reduced to smaller amplitudes for low $|\alpha|$:

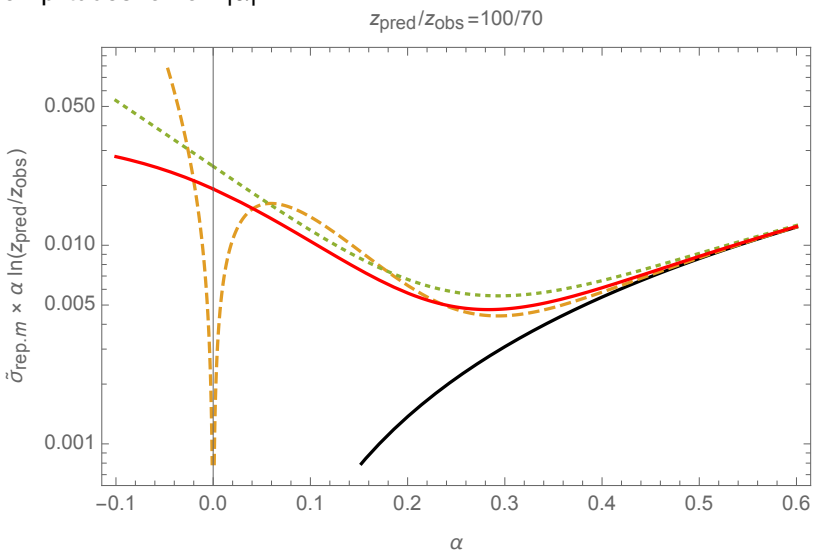

Noting that the amplitude (red line) is again the revised (final) form

$$B_{os}[1 + \tanh(-\alpha/\alpha_{\text{ref}})] \times |\alpha|^{-1} \qquad \text{(A3)}$$

with $B_{os} = 0.055$ and $\alpha_{\text{ref}} = 0.2$.

I should point out again that one *should not be alarmed by the seemingly large values* of $\tilde{\sigma}_{\text{rep}}$ for zero/small shear: recall that this is dimensionless uncertainty, which will be multiplied by the shear-extrapolation magnitude to give uncertainty (in m/s); in the end, small shear leads to small dimensional vertical-extrapolation uncertainty in wind speed, despite significant dimensionless uncertainty.

For a choice of 10% exceedance rate of predicted error over estimated uncertainty (i.e., 90$^{\text{th}}$ percentile), we obtain $B_{os} \simeq 0.4$, again with $\alpha_{\text{ref}} = 0.2$.

A.2. Measurement bias: systematic uncertainty propagation

The propagation contribution $\tilde{\sigma}_{\alpha,\mathrm{prop}}$ within the $\alpha\tilde{\sigma}_\alpha \ln(z_{\mathrm{pred}}/z_{\mathrm{obs}})$ term of (14) can be expressed

$$\alpha\tilde{\sigma}_{\alpha,\mathrm{prop}} \ln(z_{\mathrm{pred}}/z_{\mathrm{obs}}) = c_f\tilde{\sigma}_U \ln(z_{\mathrm{pred}}/z_{\mathrm{obs}}) \,/\, \ln(z_2/z_1)$$

following (11), where the $c_f = \sqrt{2}$ for uncorrelated observation uncertainty or $c_f = 2$ for fully correlated uncertainties (assuming equal uncertainty at each measurement height). This followed from $\partial U_{\mathrm{pred}}/\partial\alpha = U_{\mathrm{pred}} \ln(z_{\mathrm{pred}}/z_{\mathrm{obs}})$ multiplied by

$$\frac{\partial\alpha}{\partial U_1} = \frac{-1}{U_1 \ln(z_2/z_1)} \qquad \text{and} \qquad \frac{\partial\alpha}{\partial U_2} = \frac{1}{U_2 \ln(z_2/z_1)} \tag{A4}$$

for the case of two measurement heights, where we have thus far assumed zero-mean Gaussian errors for this $\tilde{\sigma}$ and all uncertainty components.

For *systematic* uncertainties in the wind speed observations (e.g. the measurement *biases* b_{U_1} and b_{U_2}, in contrast with the random measurement uncertainties σ_{U_1} and σ_{U_2}), the mathematical framework we've developed can again be exploited. However, for correlated measurement bias one must account for the difference in signs of the two expressions in (A4). This can be seen by writing the systematic contributions, i.e. with $\tilde{\sigma}_U$ replaced by $\tilde{b}_U$ in the above (where $\tilde{b}_{U_i} \equiv b_{U_i}/U_i$), but also including the correlated bias cross-term $\tilde{b}$:

$$\begin{aligned}
\tilde{b}^2_{\mathrm{prop}} &= \left[\left(\frac{\partial U_{\mathrm{pred}}}{\partial U_1}\right)^2 b^2_{U_1} + \left(\frac{\partial U_{\mathrm{pred}}}{\partial U_2}\right)^2 b^2_{U_2} + 2\left(\frac{\partial U_{\mathrm{pred}}}{\partial U_1}\right)\left(\frac{\partial U_{\mathrm{pred}}}{\partial U_2}\right) b_{U_1} b_{U_2} \rho_{b12}\right] / U^2_{\mathrm{pred}} \\
&= \left[\left(\frac{\partial U_{\mathrm{pred}}}{\partial\alpha}\frac{\partial\alpha}{\partial U_1}\right)^2 b^2_{U_1} + \left(\left.\frac{\partial U_{\mathrm{pred}}}{\partial U_2}\right|_\alpha + \frac{\partial U_{\mathrm{pred}}}{\partial\alpha}\frac{\partial\alpha}{\partial U_2}\right)^2 b^2_{U_2} + 2\left(\frac{\partial U_{\mathrm{pred}}}{\partial\alpha}\frac{\partial\alpha}{\partial U_1}\right)\left(\left.\frac{\partial U_{\mathrm{pred}}}{\partial U_2}\right|_\alpha + \frac{\partial U_{\mathrm{pred}}}{\partial\alpha}\frac{\partial\alpha}{\partial U_2}\right)\rho_{b12} b_{U_1} b_{U_2}\right] / U^2_{\mathrm{pred}}
\end{aligned}$$

which upon re-arranging becomes

$$\begin{aligned}
\tilde{b}^2_{\mathrm{prop}} &= \left[\frac{\ln(z_{\mathrm{pred}}/z_{\mathrm{obs}})}{\ln(z_2/z_1)}\right]^2 \left[\tilde{b}^2_{U_1} + \tilde{b}^2_{U_2} - 2\rho_{b12}\tilde{b}_{U_1}\tilde{b}_{U_2}\right] + \tilde{b}_{U_2}\left[\tilde{b}_{U_2} + 2\left(\tilde{b}_{U_2} - \tilde{b}_{U_1}\right)\frac{\ln(z_{\mathrm{pred}}/z_{\mathrm{obs}})}{\ln(z_2/z_1)}\right] \\
&= \tilde{b}^2_{U_1}\left[\frac{\ln(z_{\mathrm{pred}}/z_{\mathrm{obs}})}{\ln(z_2/z_1)}\right]^2 + \tilde{b}^2_{U_2}\left\{1 + \frac{\ln(z_{\mathrm{pred}}/z_{\mathrm{obs}})}{\ln(z_2/z_1)}\left[2 + \frac{\ln(z_{\mathrm{pred}}/z_{\mathrm{obs}})}{\ln(z_2/z_1)}\right]\right\} \\
&\qquad -2\tilde{b}_{U_1}\tilde{b}_{U_2}\frac{\ln(z_{\mathrm{pred}}/z_{\mathrm{obs}})}{\ln(z_2/z_1)}\left[1 + \rho_{b12}\frac{\ln(z_{\mathrm{pred}}/z_{\mathrm{obs}})}{\ln(z_2/z_1)}\right]
\end{aligned} \tag{A5}$$

where ρ_{b12} is the correlation coefficient between the systematic uncertainties b_{U_1} and b_{U_2}.

Thus for correlated identical measurement biases $\tilde{b}_U = \tilde{b}_{U_1} = \tilde{b}_{U_2}$ at two heights ($\rho_{b12} = 1$), the *total systematic* contribution can simply written in non-dimensional form as

$$\tilde{b}^2_{\mathrm{prop}}\big|_{\rho_{b12}=1} = \tilde{b}^2_U \,;$$

i.e. the $\tilde{\sigma}_{\alpha,\mathrm{prop}}$ component disappears. On the other hand, for *uncorrelated* biases ($\rho_{b12} = 0$), then the propagated bias is larger:

$$\tilde{b}^2_{\mathrm{prop}}\big|_{\rho_{b12}=0} = \tilde{b}^2_U\left(1 + 2\left[\frac{\ln(z_{\mathrm{pred}}/z_{\mathrm{obs}})}{\ln(z_2/z_1)}\right]^2\right).$$

References

Astrup P & Larsen SE (1999): WAsP Engineering Flow Model for Wind over Land and Sea. *Risø Report R-1107(EN)*, 1999. 24pp. ISBN 87-550-2529-3.

Irwin J S (1979): A theoretical variation of the wind profile power-law exponent as a function of surface roughness and stability. *Atmos. Environ*. **13**, 191–194.

JCGM 100:2008 (2010). GUM 1995 with minor corrections, 2010 update of "Evaluation of measurement data — Guide to the expression of uncertainty in measurement".

JCGM 101:2008 (2008). "Evaluation of measurement data – Supplement 1 to the 'Guide to the expression of uncertainty in measurements' – Propagation of distributions using a Monte Carlo method".

Kelly M, Larsen GC, Dimitrov NK, & Natarajan A. (2014): Probabilistic Meteorological Characterization for Turbine Loads. *Journal of Physics: Conference Series*. **524**, 012076 (*The Science of Making Torque from the Wind*, 2014). doi 10.1088/1742-6596/524/1/012076

Kelly M, Troen I, & Jørgensen HE (2014): Weibull-k Revisited: "Tall" Profiles and Height Variation of Wind Statistics. *Boundary-Layer Meteorology*, **152**(1), 107-124. doi 10.1007/s10546-014-9915-5

Kelly M & Troen I (2015–16): Probabilistic stability and "tall" wind profiles: theory and method for use in wind resource assessment. *Wind Energy*; **19**(2):227–241.

Kelly M & Jørgensen HE (2016). "Statistical characterization of roughness uncertainty and impact on wind resource estimation." *Wind Energy Science* **2016**-36.

Mikhail A S (1985): Height Extrapolation of Wind Data. J. Solar Energy Engineering-Transactions of the ASME **107**(1), 10–12

Triviño C, Leask P, & Beckford T (2017): Validation of Vertical Wind Shear Methods. *Journal of Physics: Conference Series* **926** (*WindEurope Conf. & Exhibition*, Session 2, 16 Mar. 2017).

Troen I, Petersen EL, and Commission of the European Communities (1989): European Wind Atlas. *Risø National Laboratory*, Roskilde, DK. 656 pp, English. ISBN: 8755014828.

Wieringa J (1989): Shapes of annual frequency distributions of wind speed observed on high meteorological masts. *Boundary-Layer Meteorology* **47**, 85–110

Acknowledgements

Bob Sherwin and Jason Fields, leadership of IEC 61400-15 committee,
whom encouraged the authors to continue with scientific and academic rigor in this work, as well as pursue membership in the IEC at the national level.

Alain Tremblay, Raghu Krishnamurthy, and Ivana Popadic, for discussions about this and related work they had undertaken.

DTU Wind Energy is a department of the Technical University of Denmark with a unique integration of research, education, innovation and public/private sector consulting in the field of wind energy. Our activities develop new opportunities and technology for the global and Danish exploitation of wind energy. Research focuses on key technical-scientific fields, which are central for the development, innovation and use of wind energy and provides the basis for advanced education at the education.

We have more than 240 staff members of which approximately 60 are PhD students. Research is conducted within nine research programmes organized into three main topics: Wind energy systems, Wind turbine technology and Basics for wind energy.

Danmarks Tekniske Universitet
DTU Vindenergi
Nils Koppels Allé
Bygning 403
2800 Kgs. Lyngby
Telephone 45 25 25 25

info@vindenergi.dtu.dk
www.vindenergi.dtu.dk